ACS OMEGA

Open Access

http://pubs.acs.org/journal/acsodf

Article

Process for Producing Lithium Iodide Cleanly through Electrodialysis Metathesis

Xu Li, Xinlai Wei,* Ningning Yang, Xuan Wang, Qun Wang, and Ke Wu

Cite This: *ACS Omega* 2024, 9, 16631−16639

Read Online

ACCESS | Metrics & More | Article Recommendations

ABSTRACT: Lithium iodide is commonly used in the production of batteries and drugs. Currently, the neutralization method is the primary means of producing lithium iodide. This method involves using hydriodic acid as a raw material, adding lithium carbonate or lithium hydroxide, and obtaining lithium iodide through evaporation and concentration. However, hydriodic acid is chemically unstable. Its preparation can lead to explosive accidents and encountering high temperatures generates toxic iodine vapors. These limitations restrict its industrial production. The study evaluates the impact of membrane stack configuration, operating voltage, and initial concentrations and volume ratios of reactants on the production process. Electrodialysis metathesis, characterized by a simpler process flow, lower energy consumption, and environmental benefits, emerges as an effective technique for electrically driven membrane separation in lithium salt production and purification. Under the specific conditions of a C−C−A−C−A−C membrane stack configuration, operating voltage at 25 V, initial potassium iodide concentration at 0.4 mol/L, initial lithium sulfate concentration at 0.2 mol/L, and a 1:1 volume ratio of product liquid to raw material liquid, the method achieves a lithium iodide purity of 98.9% with a production cost of approximately 0.502 $/kg LiI.

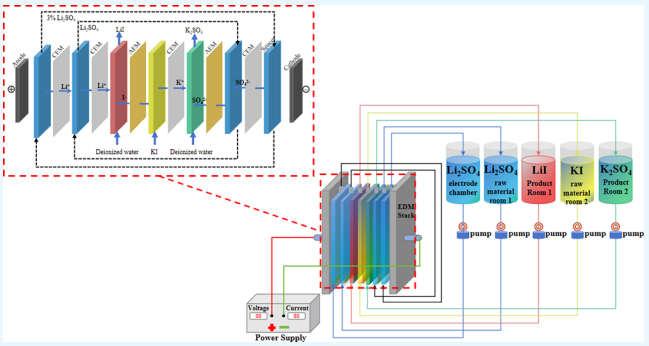

1. INTRODUCTION

Lithium iodide (LiI) is a crucial component in lithium-ion batteries, which have garnered attention in the field of new energy due to their high energy density, low energy loss, and long service life.[1,2] Lithium iodide has significant applications in medicinal chemistry. It is used to synthesize dopamine drugs and plays a role in treating Parkinson's disease, relieving symptoms such as muscle stiffness and involuntary tremors.[3] Additionally, lithium iodide is used to synthesize L-ribonucleoside, an anti-hepatitis B and HIV drug.[4,5] There are several methods for preparing lithium iodide, but most involve the use of hazardous chemicals. For example, the commonly used neutralization method involves using hydriodic acid as the raw material and adding lithium carbonate or lithium hydroxide to produce lithium iodide through a neutralization reaction. The reaction equation is as follows:

$$LiOH + HI \rightarrow LiI + H_2O$$

$$Li_2CO_3 + 2HI \rightarrow 2LiI + H_2O + CO_2\uparrow$$

The method for preparing lithium iodide in industry is often the neutralization method due to its simplicity and low cost. However, hydriodic acid, which is used in the process, is a chemically unstable and strong reducing agent that can easily be oxidized in air, resulting in the production of toxic iodine vapors. Additionally, it can decompose in light and may cause explosions during its preparation, which limits its industrialized production. It is important to find an environmentally friendly and efficient process for preparing lithium iodide.

Electrodialysis metathesis (EDM) represents an innovative membrane separation technology that amalgamates electrodialysis with metathesis principles.[6,7] Due to its unique capacity for ion recombination and concentration, EDM has emerged as a burgeoning area of research interest.[8,9] This membrane reactor system employs an alternating arrangement of anion exchange and cation exchange membranes, distinguishing it from conventional electrodialysis, comprising two raw material chambers and two product chambers.[10] Guided by an electric field force and the selective permeability of ion exchange membranes, ions within the solution migrate between adjacent compartments, resulting in a metaplasia-like reaction within the product chamber, yielding new salts.

Received: January 19, 2024
Revised: March 12, 2024
Accepted: March 15, 2024
Published: March 25, 2024

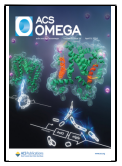

EDM can reduce energy consumption, enhance product purity, streamline purification processes, boost production efficiency, lower production costs, and, to some extent, mitigate the risk of membrane contamination.[9,11−13] Its initial application involved the production of a chlorine-free potassium fertilizer, leveraging its unique ion displacement capabilities. Zhang et al.[10] pioneered a continuous synthesis process for high-purity KNO_3, achieving remarkable production metrics, including an energy consumption of 0.165 kWh/kg KNO_3, a current efficiency of up to 94.10%, and compliance with relevant national standards. Significantly, the production cost of \$622.10/t of KNO_3 markedly undercuts the market price of \$705/t of KNO_3. These findings underscore the substantial potential of electrodialysis metathesis technology in industrial chlorine-free potash fertilizer production, garnering widespread attention due to its exceptional synthesis properties. In a study conducted by Han et al.[14] the suitability of electrodialysis metathesis for producing chlorine-free potassium fertilizer was demonstrated. They achieved this by employing electrodialysis metathesis to facilitate the conversion of KCl with acid salts (such as nitrate, carbonate, and sulfate). Furthermore, the research delved into comparing the impacts of $MgSO_4$, Na_2SO_4, and $(NH_4)_2SO_4$ on the performance of electrodialysis metathesis. To reduce wastewater pollution, Liu et al.[15] used electrodialysis metathesis to treat industrial wastewater. They employed continuous electrodialysis metathesis technology to convert the Na_2SO_4 wastewater into a high concentration of K_2SO_4. Camacho et al.[16] applied electrodialysis metathesis technology to desalinate seawater and concentrated brine, overcoming the scaling limitations of traditional electrodialysis. They achieved complete desalination of concentrated brine without the formation of precipitates in the membrane stack. Given these findings and insights, the application of electrodialysis metathesis technology in the production of lithium iodide holds the promise of enhancing efficiency, reducing costs, and fostering environmentally friendly production practices. Consequently, it emerges as a compelling and forward-looking alternative to traditional production methodologies.

Our research endeavors encompassed designing and constructing an electrodialysis metathesis membrane reactor system tailored to produce lithium iodide, utilizing potassium iodide and lithium sulfate as the primary raw materials. The metathesis reaction, characterized by the equation $2KI + Li_2SO_4 = 2LiI + K_2SO_4$, served as the cornerstone of our approach. Throughout our investigations, we systematically examined the influence of key variables, including membrane stack configuration, operating voltage, initial volume ratio of the product liquid to feedstock liquid, and initial feedstock liquid concentration, on the experimental process. We conducted a comprehensive evaluation and economic analysis of the lithium iodide products and the associated preparation process in tandem with our experimental work. Our findings and insights from this study are poised to provide valuable reference points for efficiently producing and preparing high-value lithium salt using electrodriven membrane separation technology.

2. EXPERIMENTAL SECTION

2.1. Materials. Potassium iodide (KI) and lithium sulfate monohydrate ($Li_2SO_4·H_2O$) were procured from Sinopharm Chemical Reagent Co., LTD, and these materials were of analytical purity. Deionized water was utilized for all laboratory experiments. Cation exchange membrane (CEM) and anion exchange membrane (AEM) were supplied by Hefei Kejia Polymer Material Technology Co., LTD, and their primary characteristics are detailed in Table 1.

Table 1. Ion Exchange Membrane Main Properties[a]

membrane properties	CEM	AEM
ion exchange capacities (mmol/g)	0.8−1.0	0.9−1.0
thicknesses (mm)	0.19 (±0.2)	0.15 (±0.1)
resistive (Ω·cm^2)	3.0 (±0.5)	1.5−1.8
migration number (%)	>93	95−98

[a]Data provided by the manufacturer.

2.2. Experiment Setup. A self-assembled membrane stack was used for the experiment, and the schematic diagram of the device is shown in Figure 1. The membrane stack consists of five compartments, From left to right are anode plate, electrode chamber (Li_2SO_4), CEM, raw material Chamber 1 (Li_2SO_4), CEM, product chamber 1 (LiI), AEM, raw material chamber 2 (KI), CEM, product chamber 2 (K_2SO_4), AEM, raw material chamber 1 (Li_2SO_4), CEM, electrode chamber (Li_2SO_4), and cathode plate. The effective area of each membrane is 18 cm^2, and 10 mm thick partitions separate the adjacent membranes. The cathode plate and anode plate are made of a ruthenium−titanium plate with a surface area of 18 cm^2.

A peristaltic pump (BT100S, China Baoding Lead Liquid Technology Co., Ltd.) circulated the solution through the compartments within a closed loop in the experimental setup. The electrode plate was connected to a DC power supply (WYL1703, Hangzhou Siling Electric Instrument Co., Ltd.) to supply and record the current and voltage data. The DDBJ-350 portable conductivity meter from INESA Scientific Instruments Ltd. was used to monitor the conductivity levels within raw material room 2 and product room 1. To maintain a consistent experimental temperature of approximately 25 °C, the product and raw material tank were placed in a constant temperature water bath. Initially, all solutions were set at an initial volume of 200 mL. Before commencing the experiment, feedstock room 1 was filled with Li_2SO_4 solution, while feedstock room 2 was filled with KI solution. Deionized water was subsequently introduced into both product rooms 1 and 2. The solution was pumped into the membrane stack before the current was applied to ensure proper circulation and to eliminate air bubbles within the experimental setup. The solution flow rate in each chamber was set at 300 mL/min. The experiment was concluded once the conductivity of raw material chamber 2 reached a value of 0.5 mS/cm.

2.3. EDM Membrane Stacks Preferred. In preliminary experiments using a four-compartment electrodialysis membrane stack, it was observed that iodide ions, being reductive, tend to oxidize at the positive pole of the power supply, especially at low concentrations. This oxidation was evidenced by a change in the color of the solution in raw material chamber 1, accompanied by an unpleasant odor. Further, adding a 5% starch solution to this chamber resulted in a blue-violet color change, suggesting the formation of iodine monomers. This phenomenon is likely due to the concentration difference across the interfacial layer, leading to the migration of some iodine ions through the cation exchange membrane to the positive pole, where they undergo oxidation. The presence of iodine monomers reduces the purity of the

https://doi.org/10.1021/acsomega.4c00643
ACS Omega 2024, 9, 16631−16639

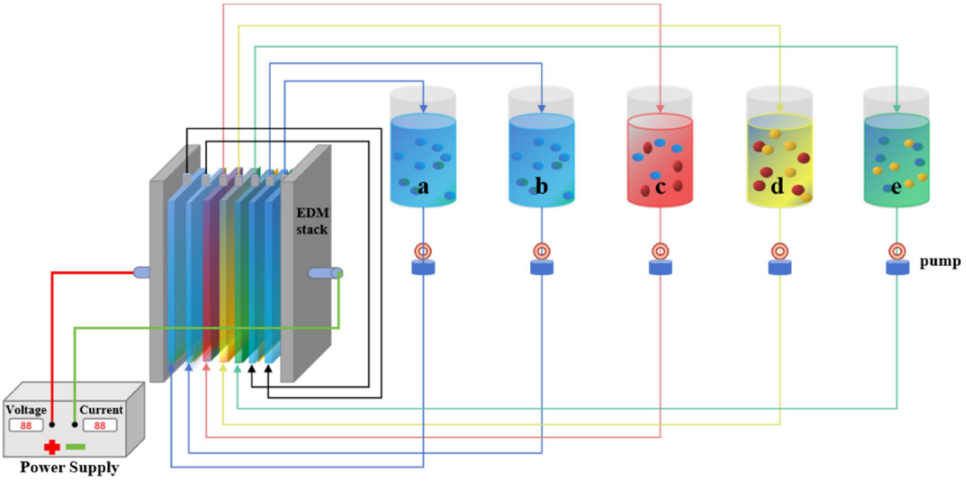

Figure 1. Schematic diagram of device operation. (a) Electrode solution tank (Li_2SO_4); (b) raw material tank 1 (Li_2SO_4); (c) product canister 1 (LiI); (d) raw material tank 2 (KI); and (e) product canister 2 (K_2SO_4).

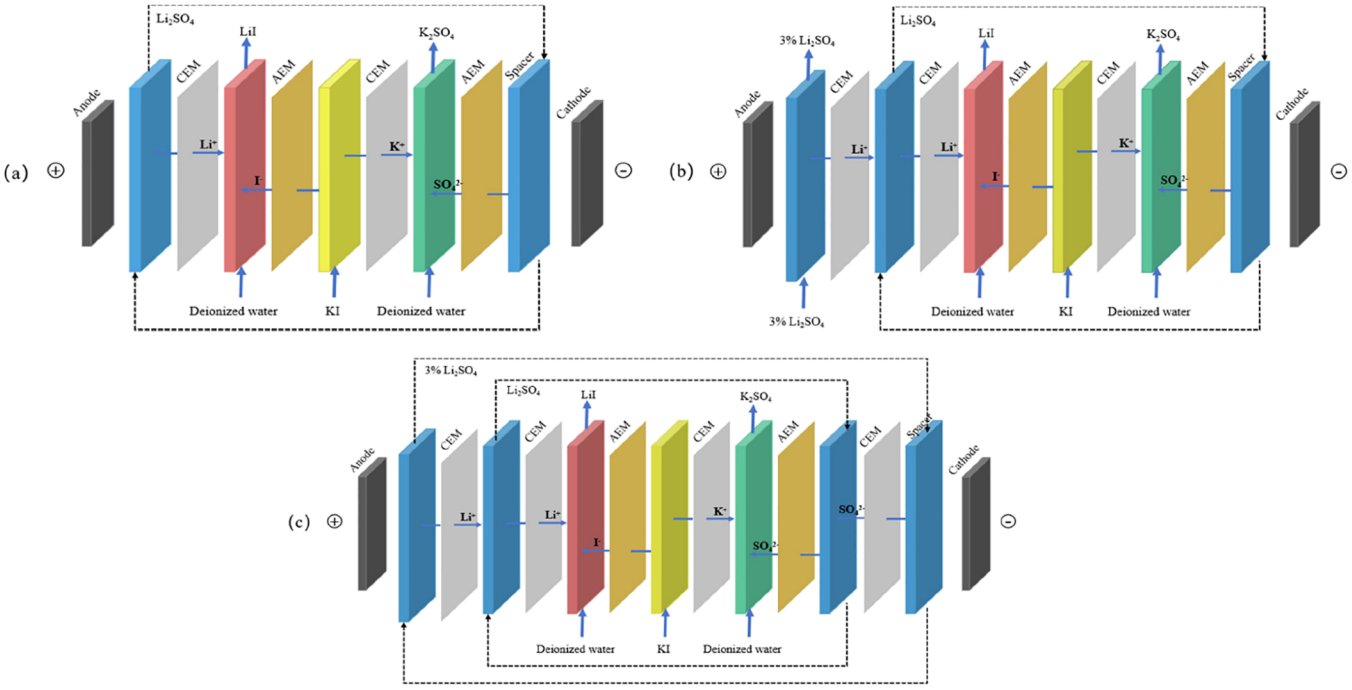

Figure 2. Three EDM membrane stack configurations. (a) C−A−C−A configuration; (b) C−C−A−C−A configuration; and (c) C−C−A−C−A−C configuration.

final product and poses potential risks to human health and electrodialysis equipment due to their toxicity and corrosiveness. Consequently, optimizing the configuration of the electrodialysis metathesis membrane stack is essential to prevent the formation of these iodine monomers.

To mitigate the formation of impurity iodine monomers, this experiment employed three distinct membrane stack configurations as depicted in Figure 2. Configuration C−A−C−A (Figure 2a) comprises four compartments. Here, I^- migrates from feed chamber 2 to product chamber 1 through the cathode membrane, driven by the electric field; as the I^- concentration increases in product chamber 1, a portion leaks into feed chamber 1 through the anode membrane, influenced by the concentration gradient in the boundary layer and the electric field, leading to oxidation at the positive electrode and iodine monomer formation. The five-compartment configuration C−C−A−C−A (Figure 2b) adds a cation exchange membrane adjacent to the power supply's positive pole, creating an anodic electrode chamber to prevent I- from feed chamber 1 from reaching the positive pole. The configuration C−C−A−C−A−C (Figure 2c) is similar to that of C−C−A−C−A, with an additional cationic membrane at the negative pole, forming an electrode chamber. These two electrode chambers are connected via a tube, enabling a circulation path. These membrane stacks were assessed for their efficacy in preventing iodine monomer formation during electrodialysis metathesis. The C−C−A−C−A−C configuration proved superior, yielding higher purity LiI products and maintaining neutral solution conditions in each compartment, enhancing equipment stability and longevity.

2.4. Analysis and Calculation. Determination of the concentration of lithium ions in product tank 1 (Figure 1c) by

https://doi.org/10.1021/acsomega.4c00643
ACS Omega 2024, 9, 16631−16639

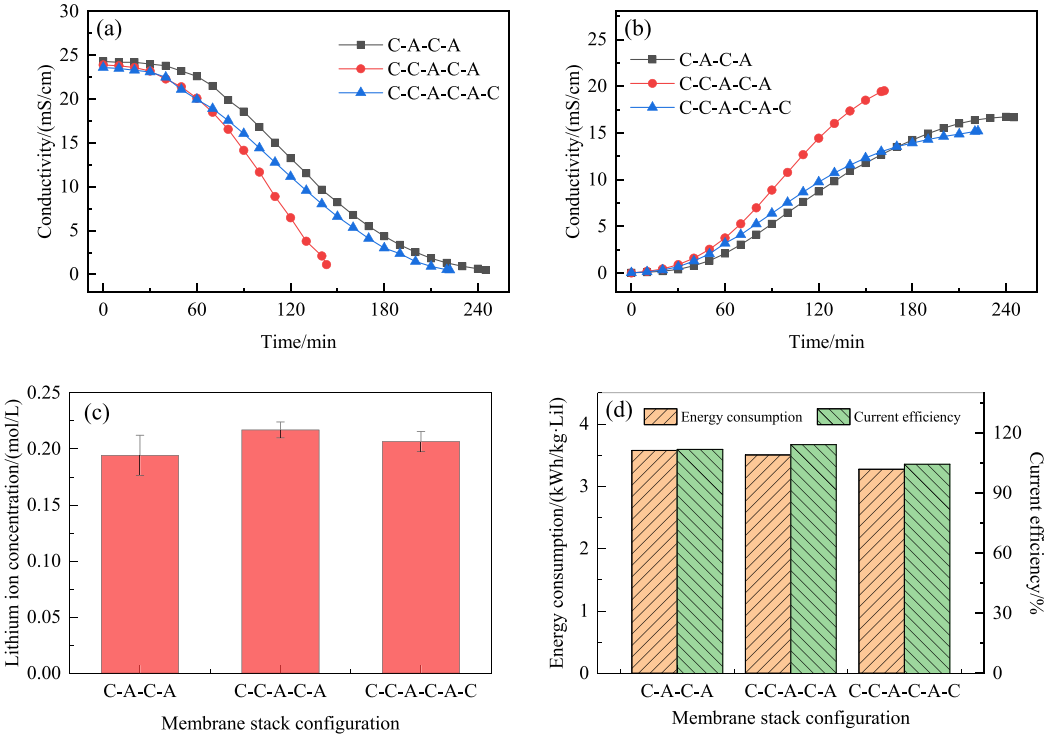

Figure 3. Effect of membrane stack configuration: (a) Feedstock chamber 2 conductivity; (b) product chamber 1 conductivity; (c) lithium ion concentration in product chamber 1; and (d) energy consumption and current efficiency.

a flame spectrophotometer (AAS Zeenit 700, Analytical Instruments AG, Jena, Germany). Iodide concentration was determined using a UV spectrophotometer. Parameters such as energy consumption (E) and current efficiency (η) are important evaluation indices and are calculated as follows:

Energy consumption (kWh/kg·LiI) was calculated according to eq 1:[17]

$$E = \int_0^t \frac{UI\,dt}{C_t V_t M} \tag{1}$$

where C_t is the molar concentration of LiI in product chamber 1 at time t, mol/L; V_t is the volume of product chamber 1 at time t, L; M is the molar mass of LiI, g/mol; U and I are the membrane stack voltage and current, V and A, respectively.

The current efficiency was calculated according to eq 2:[17]

$$\eta = \frac{zFC_tV_t - C_0V_0}{N\int_0^t I\,dt} \tag{2}$$

where z is the ionic valence state, z = 1; F is the Faraday constant, F = 96,500 C/mol; C_t and C_0 are the molar concentration of LiI in the product chamber 1 at the time t and the molar concentration of LiI in the product chamber 1 at the initial time, mol/L; V_t and V_0 are the volume of the product chamber 1 at the time t and the volume of the product chamber 1 at the initial time, L; N is the number of repetition units, N = 1; I is the current, A.

3. RESULTS AND DISCUSSION

3.1. Membrane Stack Configuration. The separation results for the three different membrane stacks are depicted in Figure 3. In this experiment, the initial concentration of KI was 0.2 mol/L, the initial concentration of Li_2SO_4 was 0.1 mol/L, and the electrode chamber was a 3% lithium sulfate solution. We investigated the effect of different membrane stacks on the preparation process. In the case of membrane stack C−A−C−A, as observed in Figure 3a,b, the conductivity of raw material chamber 1 (KI) exhibited a gradual decline (Figure 3a). In contrast, the conductivity of product chamber 1 (LiI) steadily increased (Figure 3b). This trend suggests that Li^+ ions migrated into product chamber 1. However, it is worth noting that during the experiment, a pronounced pungent odor was emitted, the color of the solution in raw material chamber 1 turned yellowish-brown, and iodine impurity monomers were detected in raw material chamber 1 and product chamber 1. These observations imply that I- ions infiltrated the electrode chamber through the anodic membrane, leading to an oxidation reaction. These phenomena collectively indicate that under the conditions of this experiment, the C−A−C−A membrane stack failed to effectively prevent the leakage of iodine ions into the electrode chamber. Consequently, the resulting impurity iodine monomer not only impairs the purity of the product but also corrodes the electrodialysis equipment.

In the case of the C−C−A−C−A membrane stack, as illustrated in Figure 3a,b, a notable trend emerges where the conductivity of feed chamber 1 (KI) decreases rapidly to 0.5 mS/cm (Figure 3a). In contrast, the conductivity of product chamber 1 (LiI) experiences a rapid increase (Figure 3b). This effect can be attributed to introducing a cation exchange membrane at the anode, forming an electrode compartment in conjunction with the cation exchange membrane. In this setup, a Li_2SO_4 solution with a concentration of 3% is pumped into the electrode compartment. Under the influence of the electric field force, Li^+ ions within the electrode compartment migrate into feed compartment 1, thereby contributing additional lithium ions to the membrane stack. This results in an enhanced current within the membrane stack and an accelerated rate of ion migration. Crucially, after the tests

https://doi.org/10.1021/acsomega.4c00643
ACS Omega 2024, 9, 16631−16639

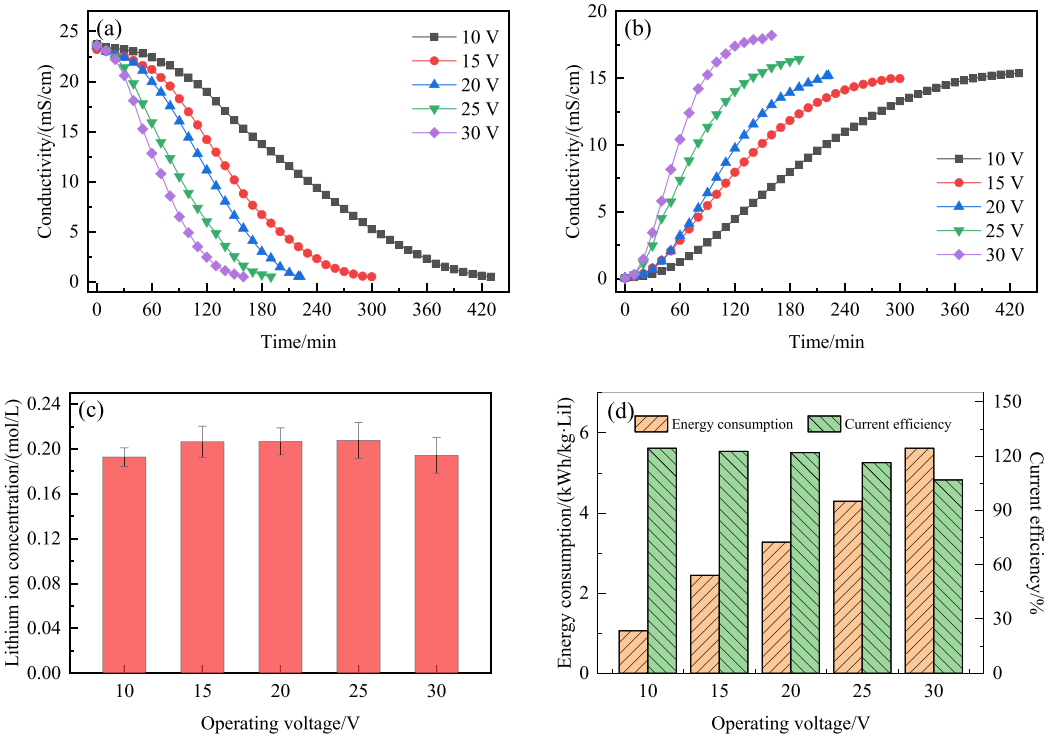

Figure 4. Effect of operating voltage. (a) Conductivity of feedstock chamber 2; (b) conductivity of product chamber 1; (c) lithium ion concentration in product chamber 1; and (d) energy consumption and current efficiency.

were conducted, it was observed that no iodine monomers were detected in either compartment. This observation signifies that the C−C−A−C−A membrane stack effectively prevented the leakage of free iodine ions into the electrode compartment by introducing an additional cation exchange membrane, thereby averting the formation of iodine monomers. However, it is important to note that because the positive and negative electrode compartments were not connected, the positive and negative electrodes of the power supply continued to generate H^+ and OH^- ions during the device's operation. This led to significant variations in the pH levels of the solutions in each compartment. Specifically, the pH levels ranged from 14, 12, 7, 12, and 2, moving from left to right across the compartments. If the C−C−A−C−A membrane stack is employed continuously, strong acid and alkali environments may lead to corrosion of the electrodialysis membrane stack. This corrosion could adversely impact the continuous and stable production of lithium iodide.

A crucial circulation flow is established between the electrode chamber and feed chamber 1 in the C−C−A−C−A−C membrane stack configuration. Importantly, the H^+ and OH^- ions generated in the electrode chamber, owing to the selective passage of the cation exchange membrane, are effectively prevented from entering the feed chamber and the product chamber. This ensured that all compartments remained neutral throughout the process. As depicted in Figure 3c, there is no discernible difference in iodide ion concentration in the final product compartment 1 (Figure 3c). This observation implies that all three membrane stack configurations can facilitate the conversion and migration of lithium ions. Figure 3d illustrates the energy consumption and current efficiency plots for the three membrane stack configurations. Notably, the C−C−A−C−A−C membrane stack exhibits the lowest energy consumption (Figure 3d). The high current efficiency observed in the C−C−A−C−A and C−C−A−C−A−C membrane stacks can be attributed to the relatively high concentration of Li_2SO_4 within the electrode chamber, which supplies additional lithium ions to the product. After the comprehensive analysis was conducted, the C−C−A−C−A−C membrane stack was ultimately selected as the preferred configuration for the clean production of LiI.

3.2. Operating Voltage. Indeed, the operating voltage plays a pivotal role in the electrodialysis metathesis process, as it directly impacts energy consumption and current efficiency within the membrane stack.[17,18] Consequently, choosing an appropriate operating voltage is of utmost significance to optimize the performance of electrodialysis metathesis. In this experiment, where the initial KI concentration was set at 0.2 mol/L and the initial Li_2SO_4 concentration was set at 0.1 mol/L, the investigation was specifically focused on understanding the influence of the operating voltage on the preparation process.

Figure 4a,b provides a visual representation of the changes in conductivity within feedstock chamber 2 (Figure 1d) and product chamber 1 (Figure 1c) at different operating voltages. As the experiment progressed, the concentration of KI in feedstock chamber 2 gradually decreased (Figure 4a), while the conductivity of product chamber 1 gradually increased (Figure 4b). This phenomenon is due to the gradual depletion of KI in raw material chamber 2. Under the action of the electric field force, iodine ions migrate to product chamber 1 through the anion exchange membrane, and potassium ions migrate to product chamber 2 (Figure 1e) through the cation exchange membrane, and the conductivity of the product chamber increases. As the operating voltage increased, the driving force also increased. This resulted in more ions passing through the ion exchange membrane per unit of time, accelerating the rate of ion migration and reducing the duration of the experimental

https://doi.org/10.1021/acsomega.4c00643
ACS Omega 2024, 9, 16631−16639

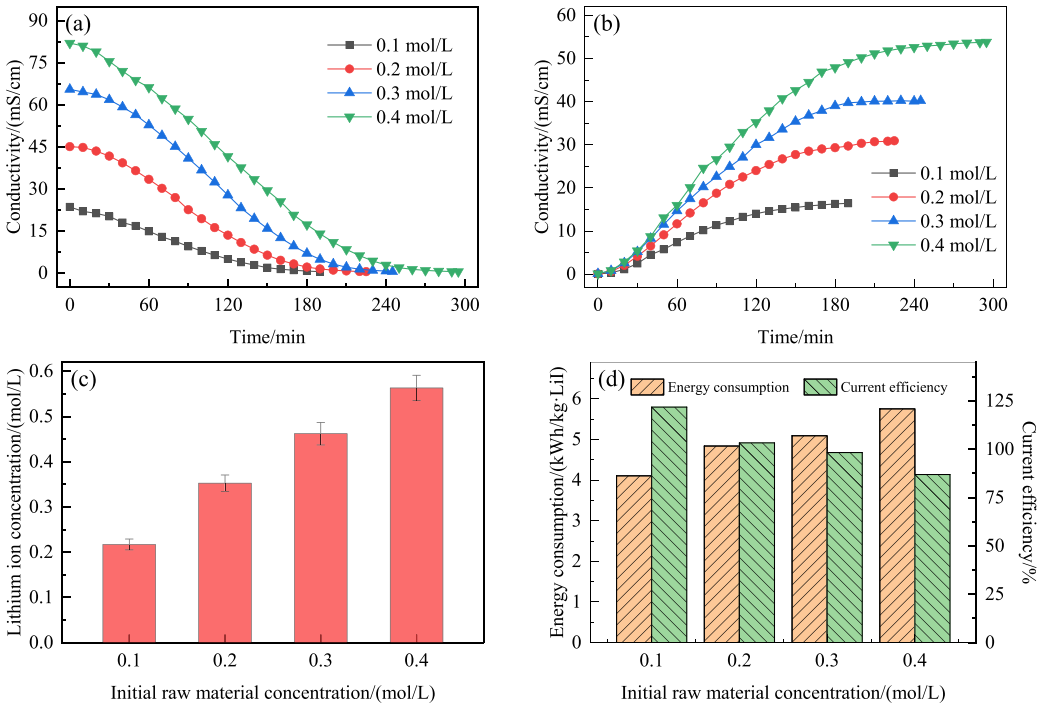

Figure 5. Effect of initial feedstock concentration. (a) Conductivity of feedstock chamber 2; (b) conductivity of product chamber 1; (c) lithium ion concentration in product chamber 1; and (d) energy consumption and current efficiency.

process. Figure 4c provides a visual representation of the lithium-ion concentration in product chamber 1 concerning the operating voltage at the end of the experiment. The lithium content in product chamber 1 remains constant as the voltage increases. This consistency can be attributed to the fixed initial concentrations of KI and Li_2SO_4 in the feedstock chamber, which can be fully converted at different operating voltages. The observed trends in conductivity, lithium-ion concentration, and membrane stack current collectively underscore the feasibility of producing lithium iodide by using the novel electrodialysis metathesis configuration.

Figure 4d depicts the impact of various operating voltages on the energy consumption and current efficiency of the electrodialysis metathesis process (Figure 4d). The energy consumption for preparing LiI per unit mass gradually escalates with the increasing operating voltage. This escalation may be attributed to intensified boundary layer concentration electrodeization and elevated membrane stack resistance that must be overcome at higher operating voltages. Higher operating voltages can also exacerbate the electrode reaction, leading to increased energy consumption.[19] The figure also reveals a slight decrease in current efficiency with rising operating voltage, likely owing to the heightened electrode reaction (Figure 4d).[20] Notably, the current efficiency may exceed 100% due to the utilization of a lithium sulfate solution with a concentration of 3% in the electrode chamber, surpassing that of raw material chamber 1. This concentration gradient induces the migration of lithium ions from the electrode chamber to the raw material and product chambers during electrodialysis, resulting in a high current efficiency within the membrane stack.

3.3. Initial Feedstock Liquid Concentration. Increasing the concentration of the initial feedstock liquid theoretically leads to a higher quantity of lithium ions migrating from the feedstock chamber to the product chamber.[21] Consequently, this increase should result in a higher final product concentration. During the experiments, the operating voltage remained fixed at 25 V. The initial concentration ratio of lithium sulfate to potassium iodide was maintained at 1:2, as per the stoichiometric equation. The effect of the initial feedstock liquid concentration on the electrodialysis metathesis performance was investigated by varying the initial lithium sulfate concentration within the range of 0.1−0.4 mol/L.

Figure 5a,b provides visual representations that support the continuous migration and decrease of KI in feedstock chamber 2 (Figure 1d), concomitant with a gradual increase in the number of ions within product chamber 1 (Figure 1c). This observation aligns with the discussion in Section 2.2. Moreover, Figure 5b illuminates that elevating the initial concentration of the feedstock solution results in a higher final concentration of LiI in product chamber 1, accompanied by a proportional increase in the experimental time (Figure 5a). This finding underscores the principle that increasing the initial concentration of the feedstock liquid can enhance the final concentration of LiI in the product, with all other factors such as operating voltage and product chamber volume being constant. Additionally, as the initial feedstock liquid concentration rises, the total number of ions in the solution increases (Figure 5c). This leads to a consistent number of ions traversing the ion exchange membrane per unit of time, extending the duration of the electrodialysis metathesis process. Figure 5c further illustrates that the concentration of lithium ions in product chamber 1 at the end of the reaction gradually increases in tandem with the feed lithium ion concentration. This trend mirrors the increase in conductivity within product chamber 1 and corroborates the effect of initial feedstock liquid concentration on lithium ion concentration in the product chamber.

Figure 5d provides a graphical representation of how the initial feed liquid concentration influences the membrane

https://doi.org/10.1021/acsomega.4c00643
ACS Omega 2024, 9, 16631−16639

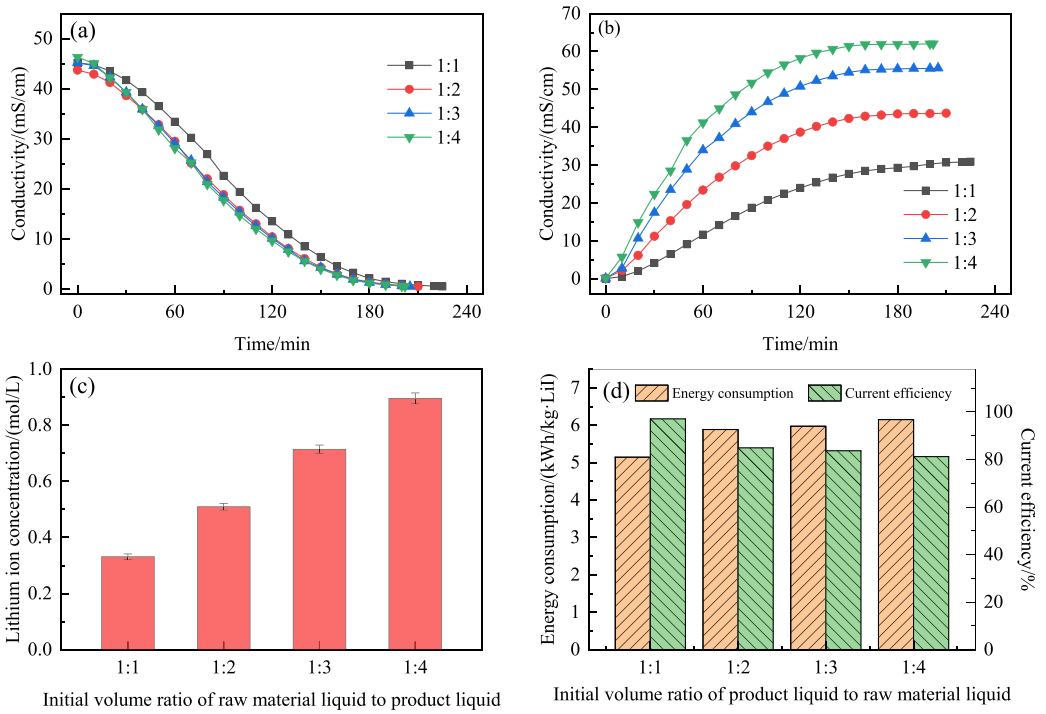

Figure 6. Effect of initial volume ratio of product to feedstock: (a) Conductivity of feedstock chamber 2; (b) conductivity of product chamber 1; (c) lithium ion concentration in product chamber 1; and (d) energy consumption and current efficiency.

reactor's energy consumption and current efficiency. The experimental findings reveal that as the initial raw material liquid concentration increases, the energy consumption gradually rises. Conversely, the current efficiency diminishes with the increase in the initial concentration. This observed phenomenon can be attributed to the increase in the concentration of the initial raw material liquid, which results in a larger concentration difference between the raw material chamber and the product chamber. Consequently, more energy is required to overcome ion diffusion, leading to an increase in energy consumption. Additionally, the heightened concentration gradient decreases the current efficiency as more energy is expended to drive the process.

3.4. Initial Volume Ratio of Product Liquid to Raw Material Liquid. Assuming a constant concentration and volume of the initial raw material liquid, the amount of lithium ions that theoretically migrate from the raw material liquid to the product liquid will remain consistent, provided that similar conversion rates are achieved. However, under intermittent operating conditions, it is possible to increase the final concentration of the product liquid by reducing the initial volume of the product liquid, effectively reducing the initial volume ratio of the product liquid to the raw material liquid. The raw material liquid was initially set at 200 mL in the experiment. The lithium iodide product liquid was prepared at 200, 100, 67, and 50 mL, respectively. Consequently, this led to initial volume ratios of product liquid to raw material liquid of 1:1, 1:2, 1:3, and 1:4. This systematic variation in the initial volume ratios allows us to explore how this parameter impacts the final concentration of the product liquid in the electrodialysis metathesis process.

Figure 6 illustrates the influence of the initial volume ratio of the product liquid to raw material liquid on the preparation process. As depicted in Figure 6a,b, the electrical conductivity of the feedstock liquid (Figure 1d) decreases with a reduction in the volume ratio, although the decrease is not highly pronounced (Figure 6a). The decrease in the volume ratio causes the ion concentration in the product chamber to increase more rapidly, resulting in a decrease in resistance and an increase in the current within the membrane stack. Consequently, the reaction time decreases and the conductivity of the raw material liquid experiences a more rapid decline. Figure 6c exhibits a significant increase in the lithium iodide product concentration within product chamber 1 (Figure 6c). This substantial rise can be attributed to the exponential reduction in the initial volume of the product liquid, leading to a faster concentration increase rate.

Figure 6d explains how the initial volume ratio of product liquid to feedstock liquid impacts energy consumption and current efficiency (Figure 6d). The figure clearly illustrates that energy consumption increases as the volume ratio decreases. This phenomenon is a consequence of reducing the initial volume of product chamber 1, which results in a rapid increase in the concentration of lithium iodide throughout the experiment. During the same reaction period, if the volume of product chamber 1 is smaller, then the concentration difference between the product and the raw material liquid becomes more significant. This elevated concentration gradient leads to a higher mass transfer resistance, making it more challenging for ions to migrate from the raw material chamber to the product chamber. Consequently, this increases energy consumption and decreases the current efficiency within the electrodialysis metathesis process.

3.5. Product Evaluation and Economic Analysis. To demonstrate the advantages of electrodialysis metathesis in the production of lithium iodide and provide valuable technical guidance for industrial applications, an evaluation of the purity and process cost of lithium iodide production through electrodialysis metathesis was conducted. The experiment was conducted with an operating voltage of 25 V, utilizing an

https://doi.org/10.1021/acsomega.4c00643
ACS Omega 2024, 9, 16631−16639

initial concentration of 0.4 mol/L for potassium iodide and 0.2 mol/L for lithium sulfate while maintaining an initial volume ratio of product liquid to raw material liquid at 1:1. As shown in Table 2, the content of various ions in product chamber 1 was measured. The results indicated that the purity of lithium iodide reached an impressive 98.9%.

Table 2. Composition of Product Room 1 (mg/L)

product	K^+	Li^+	SO_4^{2-}	I^-
LiI	99.5	2050.0	381.0	43108.9

Table 3 presents the economic analysis of the lithium iodide preparation using the electrodialysis metathesis method.

Table 3. Economic Analysis of the Production of Lithium Iodide by Electrodialysis Metathesis

parameters	EDM process	note
operating voltage (V)	25	
feed volume (L)	0.20	
salt concentration in feed chamber (g/L)	25.59	
reaction time (h)	3.75	
effective membrane area (cm^2)	108	
energy consumption (kWh/kg)	5.15	
processing capacity (kg/year)	24.46	20 h/day × 340 days
electricity costs ($/kWh)	0.09	average tariffs for industrial electricity
membrane price ($/$m^2$)	82.0	domestic membrane
membrane life and equipment amortization (year)	5.0	
membrane cost ($)	0.89	
membrane stack cost ($)	1.34	×1.5 membrane cost
peripheral equipment cost ($)	2.01	×1.5 membrane stack cost
total investment cost ($)	3.35	membrane stack cost + peripheral equipment cost
instalment price ($/year)	0.67	5 years
rate ($/year)	0.027	4.0%
maintenance cost ($/year)	0.335	10% of total investment cost
fixed cost ($/year)	1.032	
total fixed cost ($/kg LiI)	0.042	
total energy cost ($/kg LiI)	0.460	
total process cost ($/kg LiI)	0.502	total fixed cost + total energy cost

According to empirical calculations,[22,23] under optimized operating conditions, the total energy cost was estimated at 0.46 $/kg LiI, the total fixed cost at 0.042 $/kg LiI, and the total process cost at 0.502 $/kg LiI (Table 3). Furthermore, it is worth noting that in industrial-scale production, the electrode reaction constitutes a relatively small proportion of the overall process within the membrane stack. Consequently, the actual energy consumption and total production cost on an industrial scale are expected to be lower than the figures calculated in this study. This suggests that the production of lithium iodide via electrodialysis metathesis is economically feasible and holds significant potential for industrialization.

4. CONCLUSIONS

This study successfully designed and constructed a novel electrodialysis metathesis membrane reactor system based on a traditional four-compartment setup. The system utilized primary lithium sulfate as the raw material to produce high-purity lithium iodide in a single step. The research explored the effects of operating voltage, initial concentration of raw material liquid, and initial volume ratio of the product liquid to raw material liquid on the performance of electrodialysis metathesis. An evaluation and economic analysis of lithium iodide products were carried out, leading to the following conclusions:

1. The C−C−A−C−A−C membrane stack configuration effectively prevented the production of iodine, enhanced product purity, and extended the equipment's service life.
2. Operating voltage significantly influenced the performance of electrodialysis metathesis. Increasing the voltage reduced the reaction time, leading to higher energy consumption and decreased current efficiency.
3. Decreasing the initial volume ratio of product liquid to raw material liquid increased the concentration of lithium iodide but also raised energy consumption while decreasing current efficiency.
4. The concentration of lithium iodide can be increased by elevating the initial concentration of the raw material liquid. For example, at an initial concentration of lithium sulfate of 0.1 mol/L, the energy consumption was 4.1 kWh/kg.
5. High product purity, reaching 98.9%, was achieved under the conditions of a 25 V operating voltage, an initial concentration of potassium iodide of 0.4 mol/L, an initial concentration of lithium sulfate of 0.2 mol/L, and an initial volume ratio of product liquid to raw material liquid of 1:1. The estimated total cost of the process was 0.502 $/kg LiI.

These findings collectively demonstrate the feasibility and potential economic viability of producing high-purity lithium iodide through electrodialysis metathesis, offering valuable insights for industrial applications in lithium salt production.

AUTHOR INFORMATION

Corresponding Author

Xinlai Wei − *School of Biology, Food and Environment, Hefei University, Hefei 230601, China;* orcid.org/0000-0002-8522-0808; Email: weixinlai@hfuu.edu.cn

Authors

Xu Li − *School of Biology, Food and Environment, Hefei University, Hefei 230601, China;* orcid.org/0009-0003-4174-7370

Ningning Yang − *School of Biology, Food and Environment, Hefei University, Hefei 230601, China*

Xuan Wang − *School of Biology, Food and Environment, Hefei University, Hefei 230601, China*

Qun Wang − *School of Biology, Food and Environment, Hefei University, Hefei 230601, China*

Ke Wu − *School of Biology, Food and Environment, Hefei University, Hefei 230601, China*

Complete contact information is available at: https://pubs.acs.org/10.1021/acsomega.4c00643

https://doi.org/10.1021/acsomega.4c00643
ACS Omega 2024, 9, 16631−16639

Author Contributions

X.L.: Investigation and writing-original draft; X.W.: Conceptualization, writing-review, and funding acquisition; N.Y.: Writing-data and curation; X.W.: Formal analysis; Q.W.: Methodology; K.W.: Supervision, funding acquisition.

Notes

The authors declare no competing financial interest.

■ ACKNOWLEDGMENTS

This project was supported by the National Key R&D Program of China (2020YFC1908601, 2020YFC1908602); Hefei College Talent Research Fund Project (21-22RC31); and Key University Science Research Project of Anhui Province (KJ2021A0964).

■ REFERENCES

(1) Lin, Y.; Wen, Z.; Liu, J.; et al. Constructing a uniform lithium iodide layer for stabilizing lithium metal anode. *Journal of Energy Chemistry* **2021**, *55*, 129−135.
(2) Bi, X.; Li, J.; Dahbi, M.; et al. Understanding the role of lithium iodide in lithium−oxygen batteries. *Adv. Mater.* **2022**, *34* (1), 2106148.
(3) Takekiyo, T.; Yamada, N.; Amo, T.; et al. Triiodide ion-induced inhibition of amyloid aggregate formation: A case study of α-synuclein. *J. Mol. Liq.* **2022**, *360*, No. 119446.
(4) Kumamoto, H.; Higashi-Kuwata, N.; Hayashi, S.; et al. Synthesis of novel entecavir analogues having 4′-cyano-6″-fluoromethylenecyclopentene skeletons as an aglycone moiety as highly potent and long-acting anti-hepatitis B virus agent. *RSC Adv.* **2023**, *13* (23), 15999−16011.
(5) Yuldasheva, G. A.; Argirova, R.; Ilin, A. I. Molecular Modeling of the Anti-HIV Activity Mechanism of Iodine-Containing Drugs Armenicum and FS-1. *ACS omega* **2023**, *8* (9), 8617−8624.
(6) Ran, J.; Wu, L.; He, Y.; et al. Ion exchange membranes: New developments and applications. *J. Membr. Sci.* **2017**, *522*, 267−291.
(7) Campione, A.; Gurreri, L.; Ciofalo, M.; et al. Electrodialysis for water desalination: A critical assessment of recent developments on process fundamentals, models and applications. *Desalination* **2018**, *434*, 121−160.
(8) Jaroszek, H.; Dydo, P. Potassium nitrate synthesis by electrodialysis-metathesis: The effect of membrane type. *J. Membr. Sci.* **2018**, *549*, 28−37.
(9) Li, P. F.; Chen, Q. B.; Wang, J.; et al. Converting softening nanofiltration brine into high-solubility liquid salts (HSLS) via electrodialysis metathesis: effect of membrane type. *Sep. Purif. Technol.* **2021**, *267*, No. 118619.
(10) Zhang, X.; Han, X.; Yan, X.; et al. Continuous synthesis of high purity KNO3 through electrodialysis metathesis. *Sep. Purif. Technol.* **2019**, *222*, 85−91.
(11) Rottiers, T.; Van der Bruggen, B.; Pinoy, L. Synthesis and transport of impurities in electrodialysis metathesis: Production of choline dihydrogen phosphate. *J. Membr. Sci.* **2017**, *541*, 550−557.
(12) Sharma, P. P.; Gahlot, S.; Rajput, A.; et al. Efficient and cost effective way for the conversion of potassium nitrate from potassium chloride using electrodialysis. *ACS Sustainable Chem. Eng.* **2016**, *4* (6), 3220−3227.
(13) Ochoa, G. J. R.; Santa-Olalla, G. J.; de Diego, Z. A.; et al. Isolation and purification of iminodiacetic acid from its sodium salt by electrodialysis. *J. Appl. Electrochem.* **1993**, *23* (1), 56−59.
(14) Han, X.; Yan, X.; Wang, X.; et al. Preparation of chloride-free potash fertilizers by electrodialysis metathesis. *Sep. Purif. Technol.* **2018**, *191*, 144−152.
(15) Liu, J.; Xu, F.; Yuan, J.; et al. High-value conversion of Na_2SO_4 wastewater by a continuous electrodialytic metathesis process: Effects of coexisting ions. *J. Membr. Sci.* **2020**, *615*, No. 118584.
(16) Camacho, L. M.; Fox, J. A.; Ajedegba, J. O. Optimization of electrodialysis metathesis (EDM) desalination using factorial design methodology. *Desalination* **2017**, *403*, 136−143.
(17) Gao, W.; Zhao, H.; Wei, X.; et al. A Green and Economical Method for Preparing Potassium Glutamate through Electrodialysis Metathesis. *Ind. Eng. Chem. Res.* **2022**, *61* (3), 1486−1493.
(18) Haque, M. A.; Toda, K.; Ohira, S. I. Electrodialytic Universal Synthesis of Highly Pure and Mixed Ionic Liquids. *ACS omega* **2022**, *7* (25), 21925−21931.
(19) Grigoriev, S. A.; Fateev, V. N.; Bessarabov, D. G.; et al. Current status, research trends, and challenges in water electrolysis science and technology. *Int. J. Hydrogen Energy* **2020**, *45* (49), 26036−26058.
(20) Patel, S. K.; Qin, M.; Walker, W. S.; et al. Energy efficiency of electro-driven brackish water desalination: Electrodialysis significantly outperforms membrane capacitive deionization. *Environ. Sci. Technol.* **2020**, *54* (6), 3663−3677.
(21) Zhu, M.; Tian, B.; Luo, S.; et al. High-value conversion of waste Na_2SO_4 by a bielectrode membrane electrodialysis metathesis system. *Resources, Conservation and Recycling* **2022**, *186*, No. 106556.
(22) Generous, M. M.; Qasem, N. A. A.; Akbar, U. A.; et al. Techno-economic assessment of electrodialysis and reverse osmosis desalination plants. *Sep. Purif. Technol.* **2021**, *272*, No. 118875.
(23) Wang, Y.; Zhang, Z.; Jiang, C.; et al. Electrodialysis process for the recycling and concentrating of tetramethylammonium hydroxide (TMAH) from photoresist developer wastewater. *Ind. Eng. Chem. Res.* **2013**, *52* (51), 18356−18361.

https://doi.org/10.1021/acsomega.4c00643
ACS Omega 2024, 9, 16631−16639